Provided for non-commercial research and education use.
Not for reproduction, distribution or commercial use.

This article appeared in a journal published by Elsevier. The attached copy is furnished to the author for internal non-commercial research and education use, including for instruction at the authors institution and sharing with colleagues.

Other uses, including reproduction and distribution, or selling or licensing copies, or posting to personal, institutional or third party websites are prohibited.

In most cases authors are permitted to post their version of the article (e.g. in Word or Tex form) to their personal website or institutional repository. Authors requiring further information regarding Elsevier's archiving and manuscript policies are encouraged to visit:

http://www.elsevier.com/copyright

Author's personal copy

Chemie der Erde 72 (2012) 153–166

Contents lists available at ScienceDirect

Chemie der Erde

journal homepage: www.elsevier.de/chemer

Petrographic and geochemical characteristics of Paleogene turbidite deposits in the southern Aegean (Karpathos Island, SE Greece): Implications for provenance and tectonic setting

G. Pantopoulos*, A. Zelilidis

Department of Geology, University of Patras, Greece

ARTICLE INFO

Article history:
Received 2 January 2011
Accepted 22 May 2011

Keywords:
Provenance
Petrography
Geochemistry
Turbidites
Karpathos
Greece

ABSTRACT

The provenance and depositional setting of Paleogene turbidite sediments from the southern Aegean are investigated using petrography and whole-rock geochemistry. Petrography indicates that Karpathos Island turbidites are consisting of compositionally immature sandstones (graywackes–litharenites) derived from igneous (plutonic–volcanic), sedimentary, low-grade metamorphic and ophiolitic sources. The studied sediments probably reflect a mixing from an eroded magmatic arc and from quartzose, recycled sources. Major and trace element data are compatible with an acidic to mixed felsic/basic source along with input of ultramafic detritus and recycling of older sedimentary components. Geochemical data also reveal that the sediments have undergone a minor degree of weathering and no significant sediment recycling. Chondrite-normalized REE plots show a light REE enrichment (LaN/YbN ca. 7) and absence of significant negative Eu anomalies, indicating provenance from young undifferentiated arc material with contribution from an old upper continental crust source. Turbidite sedimentation probably took place in a continental island arc depositional setting as a result of subduction of a branch of Neotethys beneath a continental fragment of the Anatolide domain in Early Tertiary times. The relation of Karpathos turbidites with the Pindos foreland basin (Gavrovo and Ionian Zones of western Greece) remains problematic.
© 2011 Elsevier GmbH. All rights reserved.

1. Introduction

The southern Aegean area has received considerable geological interest in recent years due to its location near an active converged plate margin (the Hellenic Trench system), between the Hellenide and Tauride (Alpine-age) mountain chains. In southeastern Greece, the Dodecanese Islands expose geological units that are of importance in attempting to understand the Mesozoic–Cenozoic evolution and associated changing palaeogeography of the area (Harbury and Hall, 1988; Garfunkel, 2004; Kokkalas and Doutsos, 2004; Franz et al., 2005). This study focuses on the petrographic and geochemical analysis of turbidite deposits which outcrop on the Dodecanese island of Karpathos. Petrography and geochemistry of sedimentary rocks can provide a record of their provenance and the tectonic setting in which they were deposited (Dickinson and Suczek, 1979; Dickinson et al., 1983; Bhatia, 1985; Bhatia and Crook, 1986; McLennan, 1989; McLennan et al., 1990). The purpose of this study is to provide original petrographic and geochemical data from Karpathos turbidites, the processing of which will give valuable information regarding the possible ancient source areas and the depositional setting of these sediments and also will help to establish their geological setting within the southern Aegean region. Data from this study can be also used as a base for petrographic and chemostratigraphic correlations with adjacent areas of Greece and Turkey.

2. Geological setting

The pre-Neogene geological units of Karpathos (Fig. 1) are generally considered as a part of the External Hellenides (Christodoulou, 1963; Davidson-Monett, 1974; Aubouin et al., 1976; Bonneau, 1984; Fytrolakis, 1989; Kokkalas and Doutsos, 2004). However, recent geochemical and geochronological studies of Karpathos ophiolites (Koepke et al., 2002) reveal significant similarities with the Taurides ophiolites, outcropping on top of the Lycian Nappes of SW Turkey. These geological similarities between Karpathos and Lycian geology where also highlighted by Garfunkel (2004), after a palaeogeographic reconstruction of the eastern Mediterranean region. It must be noted that Bernoulli et al. (1974) have recognized typical Lycian sequences in small Dodecanese islands northwest of Karpathos. A possible fundamental change in geology between Crete and the Dodecanese Islands is also indicated by different

* Corresponding author. Tel.: +30 2610996272; fax: +30 2610996272.
E-mail addresses: george_pantop@yahoo.gr (G. Pantopoulos), A.Zelilidis@upatras.gr (A. Zelilidis).

0009-2819/$ – see front matter © 2011 Elsevier GmbH. All rights reserved.
doi:10.1016/j.chemer.2011.05.001

Author's personal copy

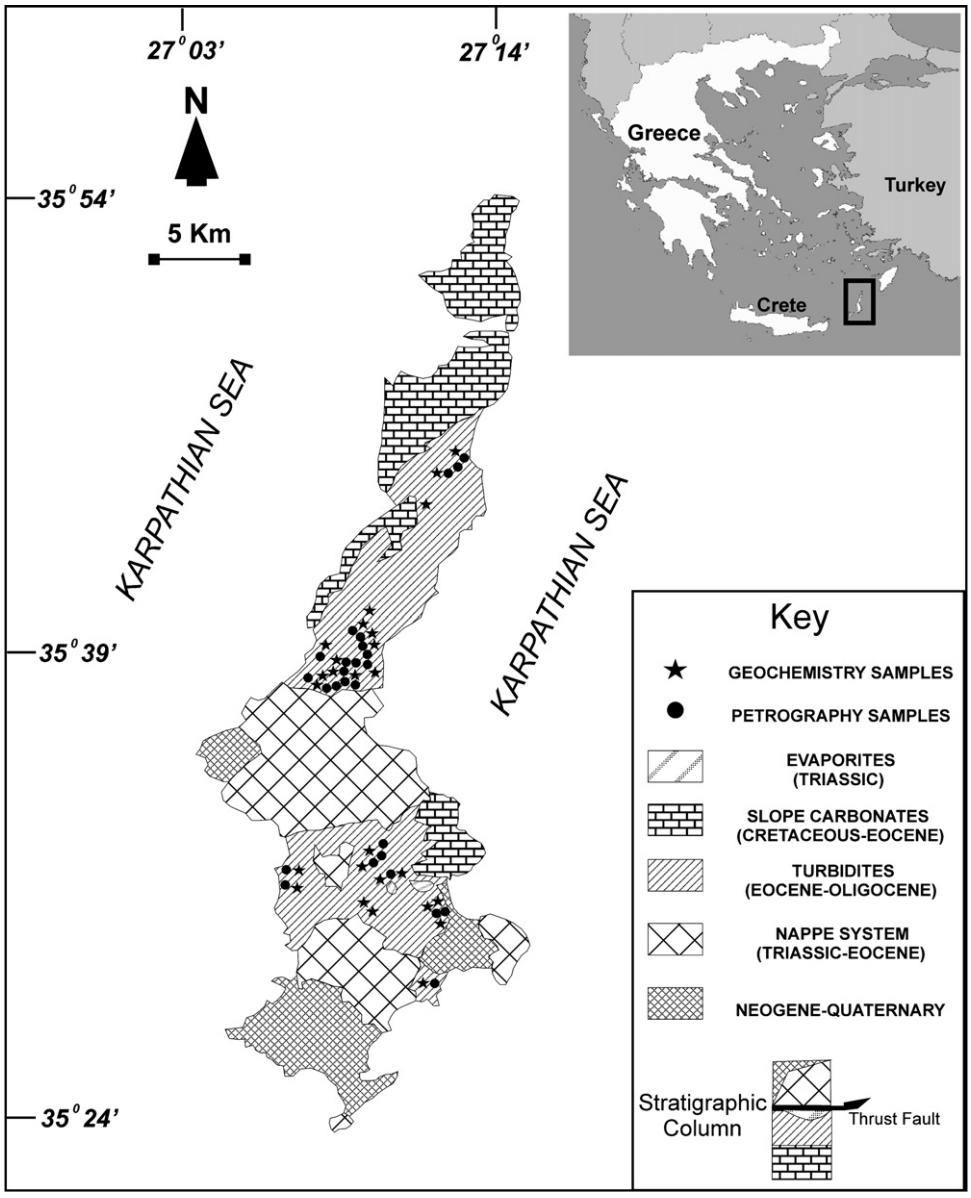

Fig. 1. Geological map of Karpathos Island (modified after Christodoulou (1963)).

inventories of the lowermost nappe units (Seidel and Wachendorf, 1986). This change conforms to a major Aegean suture separating the Hellenides in the west from the Anatolides-Taurides in the east (Langosch et al., 2000; Koepke et al., 2002; Franz et al., 2005). The turbidite deposits outcrop in two main areas of the island, one in the north and one in the south (Fig. 1). Triassic evaporites can be observed as diapirs inside the turbidites. These diapirs were probably injected into the turbidites up major faults due to tectonic deformation. Karpathos turbidites rest on carbonate slope deposits of Cretaceous to Eocene age (Harbury, 1986). The contact of the turbidites with the underlying carbonates is regionally different. Transitional deposits can be observed in northern Karpathos, but in some cases the contact is a fault. Upper stratigraphic units comprise a nappe system of Triassic to Eocene age (Fig. 1), overlying the turbidites, consisting of carbonates, cherts, volcaniclastics, molasse-type sediments and an ophiolitic mélange (Hatzipanagiotou, 1983). Recent sedimentological and biostratigraphic work on Karpathos turbidite deposits (Pantopoulos, 2009), reveals that turbidite sedimentation probably started in Early Eocene and lasted until Late Eocene–Early Oligocene. Based on sedimentological characteristics (Pantopoulos, 2009), six different turbidite units were recognized (Fig. 2): Three of them can be correlated across the island, two outcrops only in the north and one only in the south of the island. The three turbidite units that can be correlated across the island comprise of a succession of outer fan/basin plain, inner fan/channel and outer fan/olistostrome facies, from the bottom to the top (Fig. 2). The outer fan/olistostrome turbidite unit contains two main types of olistoliths composed of: a) barren micritic limestones (at the lower part of the unit) with no trace of bedding and sedimentary structures, probably originated from a pelagic sequence, b) conglomeratic, bioclastic limestones (containing rudist, mollusc, coral and algae fragments), probably derived from a shallow water area (Harbury, 1986). The units that outcrop only in the north consist of a basinal transitional carbonate/siliciclastic unit and an outer fan turbidite unit at the top of the formation. The turbidite unit at the base of the formation in the south consists of inner fan/channel facies (Pantopoulos, 2009) (Fig. 2).

Author's personal copy

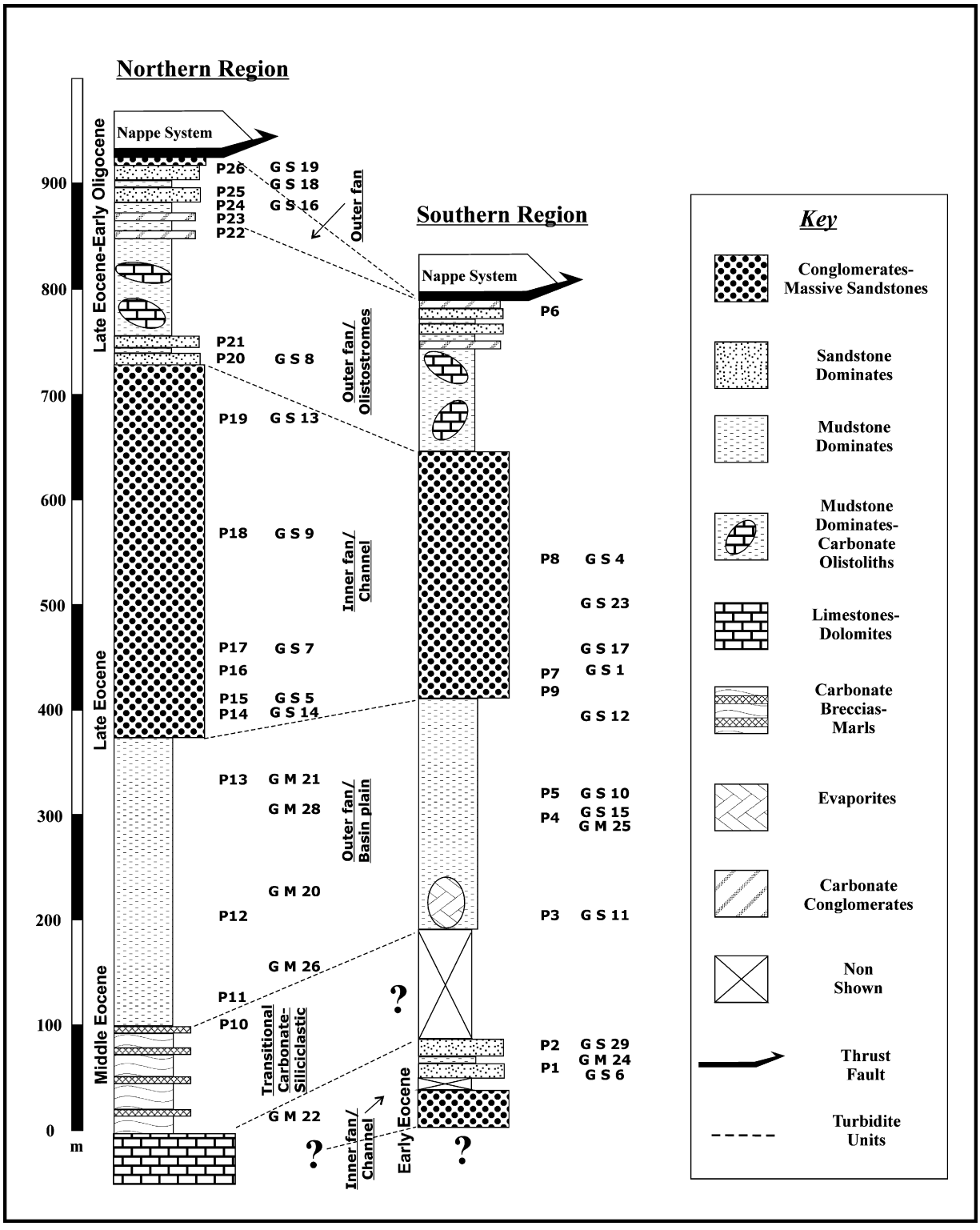

Fig. 2. Lithostratigraphic logs of the two turbidite regions of Karpathos Island. The stratigraphic position of the studied samples and the observed turbidite facies are shown (P: petrography samples, G: geochemistry samples, S: sandstones, M: mudstones).

3. Methods

Samples for petrographic analysis and whole-rock geochemistry were selected in order to cover the entire stratigraphic succession (Figs. 1 and 2; Table 1). Twenty-six fine to medium-grained, non-weathered sandstone samples were collected for petrographic analysis and polished thin sections were prepared and examined under a polarizing microscope. Framework mineral composition (modal analysis) was quantified using the Gazzi-Dickinson point-counting method (Ingersoll et al., 1984). 300 points were counted per thin section, using an automated stepping stage controlled by computer software which stores the data collected (PETROG System, Conwy Valley Systems Ltd., UK). Whole-rock geochemistry study was conducted on 26 non-weathered, mudstone and

Author's personal copy

Table 1
Coordinates of sample locations (decimal notation) taken by GPS.

Sample	Latitude	Longitude
P1/GS6/GM24	35.513611	27.197222
P2/GS29	35.514167	27.197778
P3/GS11	35.473889	27.179444
P4/GS15/GM25	35.542500	27.164444
P5/GS10	35.523333	27.117500
P6	35.532222	27.110833
P7	35.550833	27.166944
P8/GS4	35.549722	27.164722
P9	35.552778	27.163889
P10	35.757500	27.209722
P11	35.754444	27.203056
P12	35.753056	27.194444
P13/GM21	35.661111	27.156111
P14/GS14	35.658056	27.156944
P15/GS5	35.656111	27.157500
P16	35.663889	27.152222
P17/GS7	35.648611	27.132222
P18/GS9	35.645000	27.154167
P19/GS13	35.646389	27.154722
P20/GS8	35.645556	27.140833
P21	35.645833	27.141111
P22	35.645833	27.140833
P23	35.641944	27.140556
P24/GS16	35.634167	27.142500
P25	35.628333	27.127778
P26	35.636111	27.148611
GS1	35.513889	27.148611
GS12	35.542222	27.164167
GS17	35.514167	27.150556
GS18	35.638889	27.129167
GS19	35.634722	27.142500
GS23	35.550556	27.167222
GM20	35.753056	27.188889
GM22	35.737500	27.181111
GM26	35.755000	27.212500
GM28	35.675000	27.158333

Table 2
Modal analysis data of the studied sandstone samples.

Sample	Q (%)	F (%)	L (%)	Matrix (%)
P1	29.6	21.4	14.3	27.2
P2	20.2	15.6	9.9	47.5
P3	18	25	13.7	28.7
P4	29.3	15.3	10.7	41
P5	20	14.7	22.3	35
P6	8.2	32.6	26.2	22.5
P7	34	18.7	10.3	29.7
P8	20	21.1	16	33.3
P9	25.3	15.8	15.8	37.5
P10	16.3	5	5.7	69.3
P11	26.3	10.3	12	44
P12	33.3	10	30.6	10.7
P13	60.4	17.8	6.6	11.7
P14	35.3	32.3	14.3	11.5
P15	18.6	23.4	26.1	25.4
P16	24.5	24.8	19	24.1
P17	28.2	13.2	18.8	26.7
P18	27.3	33	15	14.3
P19	28	19	24.3	17.7
P20	31	22.7	16.3	24.7
P21	15.3	14.9	13.2	27.8
P22	32.4	15.4	29.6	13.8
P23	28.3	20	18.3	28.7
P24	20.5	28.3	25	20.5
P25	24	25.3	19.7	27.7
P26	33.6	39.3	10.5	12.2
Mean	26.45	17.08	20.57	27.43

fine to medium-grained sandstone samples at Activation Laboratories, Ontario, Canada. Major elements and 20 trace elements were determined using a combination of fusion ICP-OES, ICP-MS and INAA methods. A 0.25 g sample aliquot was digested with $HClO_4$–HNO_3–HCl–HF at 200 °C to fuming and was then diluted with aqua regia. Samples were then prepared and analyzed in a batch system. Each batch contained a method reagent blank, certified reference material, and 17% replicates. Samples were mixed with a flux of lithium metaborate and lithium tetraborate and fused in an induction furnace. The molten melt was immediately poured into a solution of 5% nitric acid containing an internal standard, and mixed continuously until completely dissolved. The samples were then analyzed for major oxides and selected trace elements on a combination simultaneous/sequential Thermo Jarrell-Ash ENVIRO II ICP. For the ICP/MS analysis, reagent blanks with and without the lithium borate flux were analyzed, as well as the method reagent blank. Interference correction verification standards were analyzed. Two of the standards were used during the analysis for every group of ten samples. This standard brackets the group of samples. The sample solution was also spiked with internal standards and was further diluted and introduced into a Perkin Elmer SCIEX ELAN 6000 ICP/MS using a proprietary sample introduction methodology. Calibration was performed using USGS and CANMET certified reference materials. For the INAA portion, a 1 g sample aliquot was encapsulated in a polyethylene vial and irradiated with flux wires and an internal standard (1 for 11 samples) at a thermal neutron flux of 7×10^{12} n cm^{-2} s^{-1}. After a 7-day decay to allow Na-24 to decay the samples are counted on a high purity Ge detector with resolution of better than 1.7 keV for the 1332 keV Co-60 photopeak. Using the flux wires, the decay-corrected activities are compared to a calibration developed from multiple certified international reference materials. The method is described in detail by Hoffman (1992). The abundances of eight REE (La, Ce, Nd, Sm, Eu, Tb, Yb, Lu) were also determined using INAA methods. Due to the fact that the majority of the analyzed sediments display Tb values lower than the detection limit of the method used (0.5 ppm), this particular REE has not been plotted in the chondrite-normalized (Taylor and McLennan, 1985) REE plots that were used.

4. Results

4.1. Sandstone petrography

Petrographic analysis of the selected samples shows that the major components of the studied Karpathos sandstones are: quartz and feldspar grains, metamorphic, igneous and sedimentary lithic fragments, accessory and heavy minerals, phyllosilicates and matrix. The studied sandstones are generally immature and poorly to medium sorted.

4.1.1. Quartz

Quartz is the most abundant grain component in the studied sandstones and accounts for 8.2–60.4% of the studied thin sections with a mean of 26.45% (Table 2). Both monocrystalline (Qm) and polycrystalline quartz (Qp) occurs (Fig. 3). This fact suggests derivation from both granitic and gneissic sources, as well as derivation from schists respectively (Tortosa et al., 1991). Monocrystalline quartz contains both nonundulose and undulose grains. Nonundulose quartz grains are dominant in sandstones derived from plutonic rocks, while monocrystalline quartz from low-rank metamorphic rocks contains both nonundulose and undulose grains (Basu et al., 1975). Qm is usually in the form of subangular to subrounded and occasionally well-rounded grains indicating the reworked sedimentary origin. Most of the polycrystalline quartz grains (Qp) consist of more than three crystals and have been grouped in two types: 1) polycrystalline grains composed of more than five elongated crystals exhibiting irregular to crenulated inter-crystal boundaries and 2) polycrystalline quartz grains composed of five or more crystals with straight to slightly curved inter-crystal

Author's personal copy

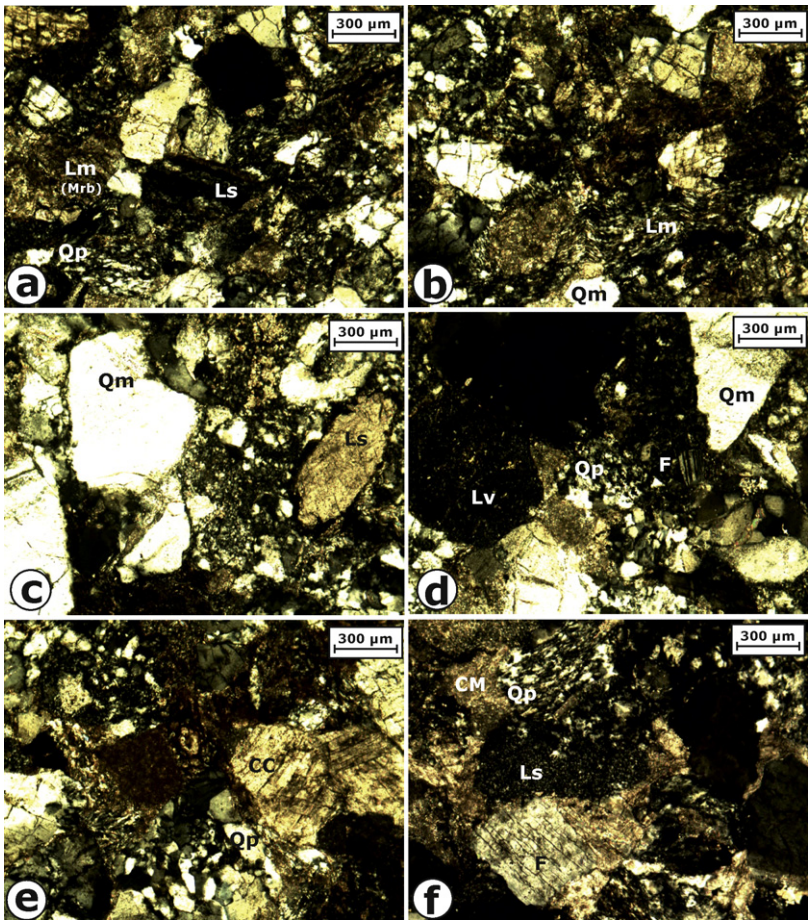

Fig. 3. Photomicrographs of the studied sandstones (crossed nicols): a) Polycrystalline quartz (Qp) grain probably belonging to a lithic fragment of metamorphic origin, along with lithic fragments of sedimentary (Ls) and metamorphic origin (Lm) (marble fragment). b) Monocrystalline quartz (Qm) grain and a lithic fragment of metamorphic origin (Lm), probably a schist rock fragment. c) Monocrystalline quartz (Qm) grain and a lithic fragment of sedimentary origin (Ls), probably a carbonate rock fragment. d) Monocrystalline (Qm) and polycrystalline (Qp) quartz grains, feldspar grain (F) and a lithic volcanic (Lv) grain, probably a basalt rock fragment. e) Polycrystalline quartz (Qp) and occurrence of carbonate cement (CC). f) Polycrystalline quartz (Qp), feldspar (F), and a lithic fragment of sedimentary origin (Ls), probably chert. Carbonate matrix (CM) is also shown.

boundaries. The first type indicates an origin from metamorphic source rocks (Blatt et al., 1980; Asiedu et al., 2000), while the second type suggests an origin from plutonic igneous rocks (Folk, 1974; Blatt et al., 1980).

4.1.2. Feldspar

Feldspar content in the studied sandstones ranges from 5.7 to 30.6% of the studied thin sections with a mean of 17.08% (Table 2) and consist of both alkali feldspar and plagioclase grains (Fig. 3). Feldspar grains may be unaltered but usually are altered to sericite, or replaced by calcite. Orthoclase is the most common alkali feldspar, but microcline can also be observed.

4.1.3. Lithic fragments

After quartz, lithic fragments constitute the most abundant framework grain component in the sandstones and account for 5–39.3% of the studied thin sections with a mean of 20.57% (Table 2). A wide range of fragments has been observed including metamorphic (Lm), sedimentary (Ls) and igneous (Li) lithic fragments (Fig. 3). Metamorphic fragments consist of mica and graphite schist, quartzite, marble, gneiss and augengneiss fragments, while sedimentary lithic fragments include microcrystalline chert, limestone, sandstone, glauconitic sandstone and mudstone fragments. Igneous lithic fragments consist of felsic plutonic granite, mafic volcaniclastic basalt and also serpentinite and dolerite (diabase) fragments (Fig. 4).

4.1.4. Heavy minerals

A limited range of heavy minerals has been observed in the studied thin sections. The most common include zircon, rutile, tourmaline and apatite grains. Several chromium spinel grains along with opaque minerals were also observed (Fig. 4).

4.1.5. Accessory minerals

The accessory minerals that have been identified in the studied sandstones include epidote and pumpellyite. The latter is probably derived from low grade metamorphism of basaltic rocks.

4.1.6. Phyllosilicates

Phyllosilicates are generally confined to the matrix and consist mainly of illite and chlorite. Small elongate grains of mica, mainly muscovite, were observed. In some sandstone samples kaemmererite (chromium-rich chlorite) was observed, in close relation with altered chromium spinel grains.

4.1.7. Matrix

Matrix content of the studied sandstones ranges from 10.7 to 69.3% with a mean of 27.43% (Table 2). It is mainly composed of calcite, but illite, chlorite, altered feldspar and lithic fragments and very fine material also contribute. In many thin sections calcite cement and iron oxides can be observed. It is uncertain as to how much of the matrix is primary and how much has been produced by the alteration of feldspars and lithic fragments. However, some of

Author's personal copy

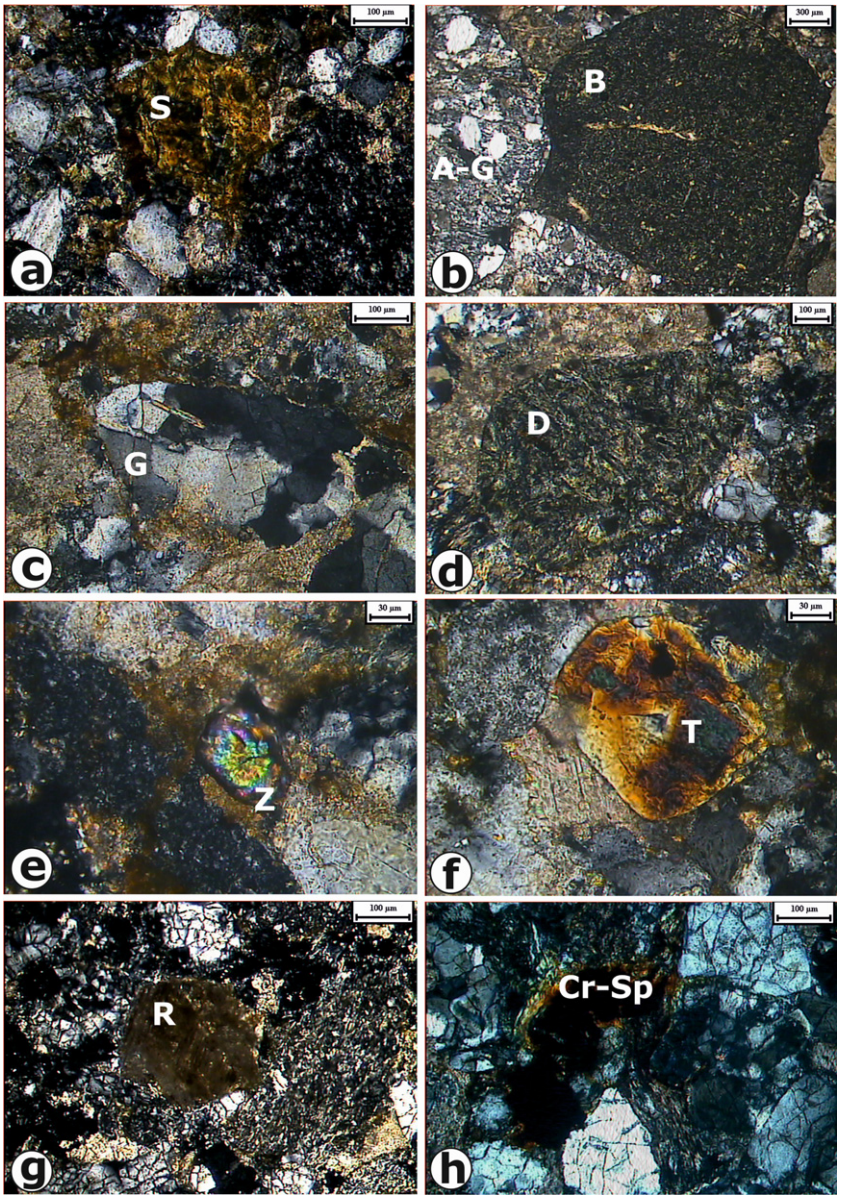

Fig. 4. Photomicrographs of the studied sandstones, in which lithic fragments and heavy mineral grains are shown (crossed nicols): a) Serpentinite (S). b) Basalt (B) and augen-gneiss (A-G). c) Granite (G). d) Dolerite (D). e) Zircon (Z). f) Tourmaline (T). g) Rutile (R). h) Chromium spinel (Cr-Sp).

the matrix is clearly "pseudomatrix" (Dickinson, 1970) representing altered detrital framework grains.

4.1.8. Tectonic setting

The determination of the tectonic setting of sandstones using the framework mineral composition (detrital modes) was first proposed by Crook (1974) and has since undergone considerable refinement (Dickinson and Suczek, 1979; Dickinson et al., 1983). Modal analysis from point-counting of the framework grains is listed in Table 2, where both monocrystalline and polycrystalline quartz (Q), total feldspar (F), total lithic fragments (including microcrystalline chert) (L) and matrix are distinguished. Plotting data from the modal analysis of the Karpathos sandstones (Fig. 5), in the ternary QFL diagram of Dickinson et al. (1983), shows that the studied sandstones cluster mainly in the dissected arc and recycled orogenic fields. One sandstone sample plots in the transitional arc field. Although care was taken to avoid alteration due to weathering by collecting only the freshest samples, high matrix content (>25%) in many samples suggests that diagenetic alteration of some grains to matrix may have occurred. In the study of Dickinson et al. (1983), samples with greater than 25% matrix are disregarded in order to prevent mistaken provenance assignment due to diagenetic changes to the modal composition. Although 14 out of the 26 studied Karpathos samples fall within this matrix limit, in order to provide data from as many samples as possible, 9 samples above this limit (with matrix content of less than 35%) have been included in the QFL ternary diagram. This approach has also been followed in previous studies (Burnett and Quirk, 2001), in the case of petrographical analysis of matrix-rich sandstones.

4.2. Sandstone/mudstone geochemistry

In general, the alkali and alkaline-earth elements can be strongly fractionated by weathering and diagenesis (Nesbitt et al., 1980), making them liable to movement and thus influencing the geochemical composition of the sediment. Therefore, geochemical analysis discrimination diagrams using such elements must be treated with caution. Immobile trace elements are expected to be

Author's personal copy

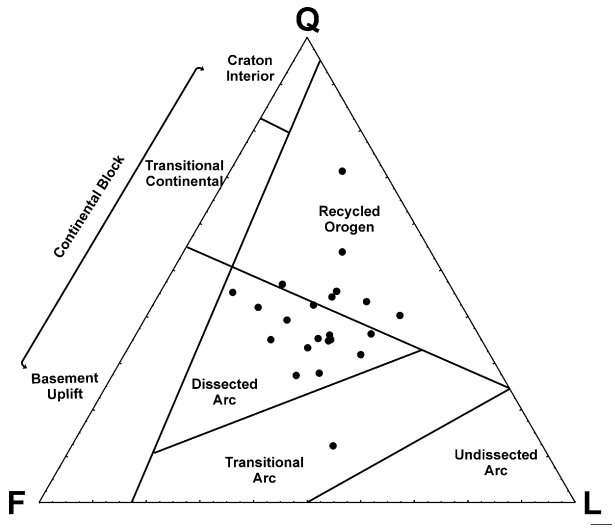

Fig. 5. QFL ternary diagram after Dickinson et al. (1983). The studied sandstones plot mainly in the dissected arc and recycled orogenic fields.

more useful in studying sedimentary provenance and depositional setting than major elements (Bhatia and Crook, 1986; McLennan et al., 1993). The REE in particular are best suited for such studies, because of their relative immobility during weathering, transport and diagenesis (McLennan, 1989). In this study, with the exception of a few major-element fingerprints, only relatively immobile trace elements and REE were used for the determination of sedimentary provenance and depositional setting.

4.2.1. Chemical classification

Various classification schemes for clastic sediments based on whole-rock chemical data have been established (Pettijohn et al., 1972; Herron, 1988). Fig. 6 shows the classification diagram of Herron (1988), which distinguishes between lithologies according to their logarithmic ratios of SiO_2/Al_2O_3 vs. Fe_2O_3/K_2O. Most of the analyzed sandstone samples are classified as unstable immature wackes (greywackes) and litharenites. The rest of the sandstones are classified as Fe-sandstones. The mudstone samples plot in the shale field of the diagram or in the shale/wacke boundary. The geochemical classification of the studied sandstone samples is broadly coincident with the petrographical observations.

4.2.2. Mineral controls on whole-rock geochemistry

Fig. 7 shows some bivariate diagrams to identify mineral controls on whole-rock geochemistry. The strong positive linear correlations between K_2O and Rb with Al_2O_3 (Fig. 7a, b) suggest that both K and Rb reside in phyllosilicates. Because mudstones are more enriched in clay minerals and/or micas than sandstones, they occupy distinct fields in Fig. 7a, b. CaO is mainly bound in carbonates as indicated by the positive correlation between CaO and LOI (Fig. 7c). Sandstone samples show a lack of correlation between Cr and Al_2O_3 (Fig. 7d) indicative of possible presence of Cr-bearing accessory oxide minerals such as chromite (Meinhold et al., 2007).

4.2.3. Weathering and sediment recycling

Fig. 8a shows the Th/U vs. Th plot of McLennan et al. (1993). In contrast to Th, U is easily mobilized during weathering and sedimentary recycling, resulting in an increase of the Th/U ratio. Upper crustal rocks have a Th/U ratio averaging around 3.8 (Taylor and McLennan, 1985). The Th/U ratios of the studied samples range from 2 to 4.41. On average, the Th/U ratio of almost all the analyzed sandstones and some mudstones lies below the value for the upper continental crust (UCC). The latter indicates that these sediments were derived from source rocks with the least weathering and/or from material with the least recycling. In contrast, two mudstone samples seem to follow the normal weathering trend. More than half of the studied sandstones lie in the field of depleted mantle sources. Their source rocks were probably non-recycled arc magmatic rocks that have undergone a minimal degree of weathering.

The compositional variation and the degree of sediment reworking and heavy mineral sorting can be illustrated in a plot of Th/Sc vs. Zr/Sc (McLennan et al., 1993). A positive linear correlation between the two ratios expresses the igneous differentiation trend. The Th/Sc ratio of sedimentary rocks characterizes the average provenance, whereas an increase in the Zr/Sc ratio alone indicates significant sediment reworking, consistent with zircon enrichment (McLennan et al., 1993). The Zr/Sc ratios are relatively smaller for most of the studied mudstones (Fig. 8b), suggesting concentration of zircon in the coarser fraction. All the studied samples seem to

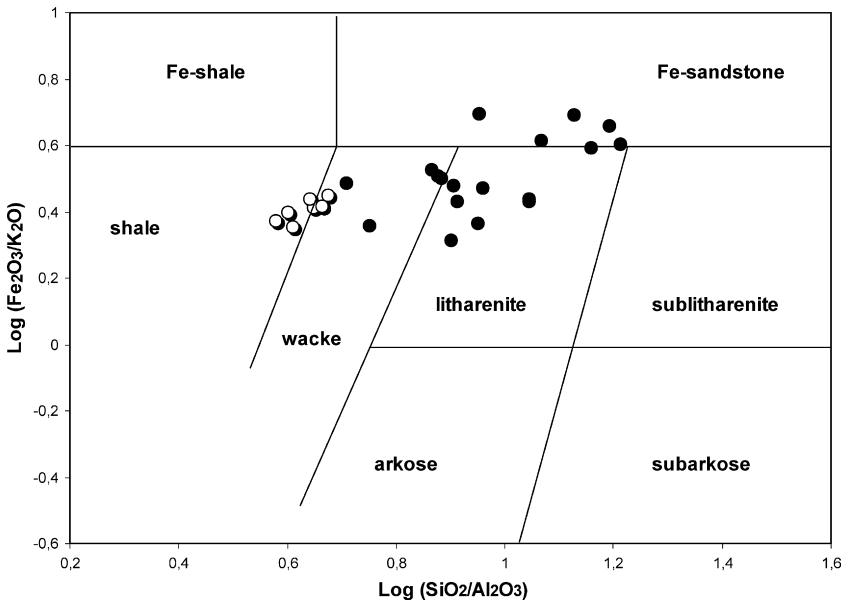

Fig. 6. Chemical classification scheme for terrigenous clastic sediments after Herron (1988). Black dots: sandstones, white dots: mudstones.

Author's personal copy

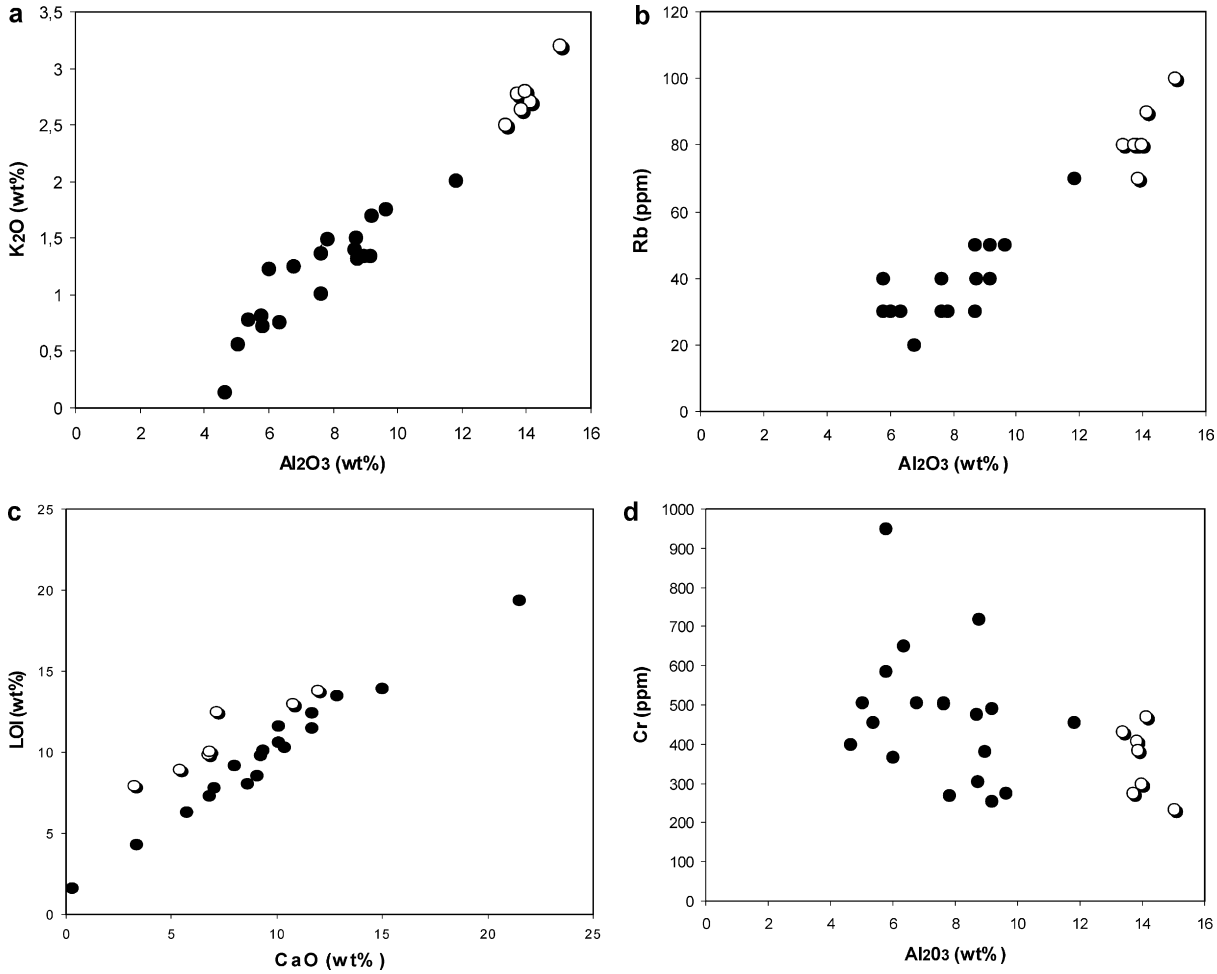

Fig. 7. Correlation diagrams of K, Rb and Cr vs. Al_2O_3 and CaO vs. LOI for turbidite sediments of Karpathos. Black dots: sandstones, white dots: mudstones.

have undergone minor degree of weathering and no significant sediment recycling.

4.2.4. Provenance

Fig. 9 summarizes various diagrams for sedimentary provenance. Roser and Korsch (1988) proposed discriminant functions (DFs) for sedimentary provenance using major-element ratios (Fig. 9a). The analyzed samples lie mainly in the fields of the DF diagram of Roser and Korsch (1988) which indicate quartzose sedimentary provenance and intermediate igneous provenance respectively. Four sandstone samples plot in the field of felsic igneous provenance.

Floyd and Leveridge (1987) established a discrimination diagram using the La/Th ratio vs. Hf to determine different arc compositions and sources (Fig. 9b). Low La/Th ratios (<5) and Hf contents of about 1.4–7.1 ppm for all the studied samples, suggest derivation from an acidic and a mixed felsic/basic arc source, with a minor influence of an old sediment component.

Plotting of Cr/V vs. Y/Ni ratios can illustrate the importance of ophiolitic provenance (Hiscott, 1984; McLennan et al., 1993). The Cr/V ratio monitors the enrichment of Cr over other ferromagnesian trace elements, whereas the Y/Ni ratio shows the general level of ferromagnesian trace elements (Ni) compared with Y, which is used as a proxy for the heavy REE (McLennan et al., 1993). Mafic-ultramafic sources tend to have higher Cr/V and lower Y/Ni ratios. Fig. 9c shows that all the samples exhibit very low Y/Ni ratios (<0.25) and half of the sandstones have a Cr/V ratio of more than 8, suggesting the existence of a mafic/ultramafic source.

Garver et al. (1996) used Cr and Ni whole-rock geochemistry of shales to identify ophiolitic rock sources. They suggested that values of Cr > 150 ppm, Ni > 100 ppm, Cr/Ni ratio of about 1.3–1.5 and a high correlation coefficient between Cr and Ni in shales, are diagnostic of ultramafic rocks in the source area, whereas higher Cr/Ni ratios (around 2 or higher) indicate mafic volcanic detritus. Cr/Ni ratios of more than 3 for sandstones suggest significant sedimentary fractionation (Garver et al., 1996). Karpathos mudstone samples have Cr/Ni ratios of 0.91–1.64 with a mean of 1.42 (Cr 234–471 ppm, Ni 189–286 ppm). The Cr–Ni signatures of the studied mudstones (Fig. 10) typify an input of ultramafic rocks from the source area. Nine sandstone samples exhibit Cr/Ni > 3 and seem to have been affected by sedimentary fractionation. Mudstones tend to have higher Ni values than sandstones (Fig. 10). The latter observation supports the suggestion of Weber and Middleton (1961a,b) that Ni is principally derived from easily disintegrated pyroxene, olivine and serpentine (Garver et al., 1996).

The degree of light REE (LREE: La-Sm) vs. heavy REE (HREE: Gd-Lu) enrichment is assessed through the ratio of chondrite-normalized (Taylor and McLennan, 1985) La and Yb values (LaN/YbN). All samples reveal LREE enrichment with an average LaN/YbN of ≈7. The Eu anomaly in clastic sediments is a good fingerprint for source rock characterization. This parameter reflects changes in a mixture between juvenile crustal influx, without negative Eu anomaly, characterizing active continental margin settings, and recycled crustal material, with significant negative Eu anomaly, characterizing evolved stable cratons (Gao and Wedepohl, 1995; Meinhold et al., 2007). Fig. 11 shows chondrite-normalized (Taylor

Author's personal copy

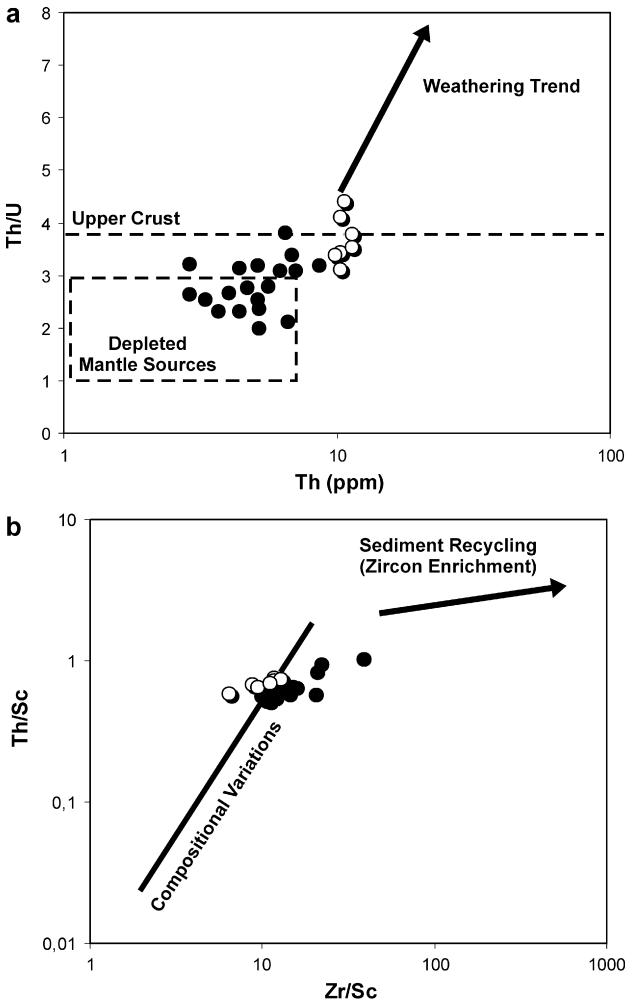

Fig. 8. Discrimination diagrams illustrating weathering and sediment recycling: a) Th/U vs. Th diagram after McLennan et al. (1993). b) Th/Sc vs. Zr/Sc diagram after McLennan et al. (1993). Black dots: sandstones, white dots: mudstones.

and McLennan, 1985) REE patterns for the studied sediments, which show that all samples exhibit either minor positive or no Eu anomalies and significant negative Eu anomalies are not observed. The lack of a negative Eu anomaly in the studied samples probably resulted from influx of material from a juvenile island arc (McLennan et al., 1993; Burnett and Quirk, 2001), or concentration of plagioclase in the sand-sized fraction during sorting (McLennan et al., 1990). The chondrite-normalized (Taylor and McLennan, 1985) REE patterns (Fig. 11) generally suggest a derivation from young undifferentiated arc material (lack of negative Eu anomalies) with contribution from old upper continental crust (LREE enrichment) (McLennan et al., 1993).

4.2.5. Tectonic setting

Trace elements with relatively low mobility and low residence time in ocean water, such as La, Th, Zr and Sc, are transferred quantitatively into clastic sediments during primary weathering and transportation, and are thus useful fingerprints for chemical discrimination of plate tectonic settings (Bhatia and Crook, 1986). The following settings are distinguished: oceanic island arc (OIA), continental island arc (CIA), active continental margin (ACM) and passive margin (PM). In the ternary diagrams of Bhatia and Crook (1986) almost all sandstones plot in the continental island arc field (Fig. 12a, b). Bhatia (1985) established several REE-related parameters to distinguish the tectonic setting of terrigenous sedimentary

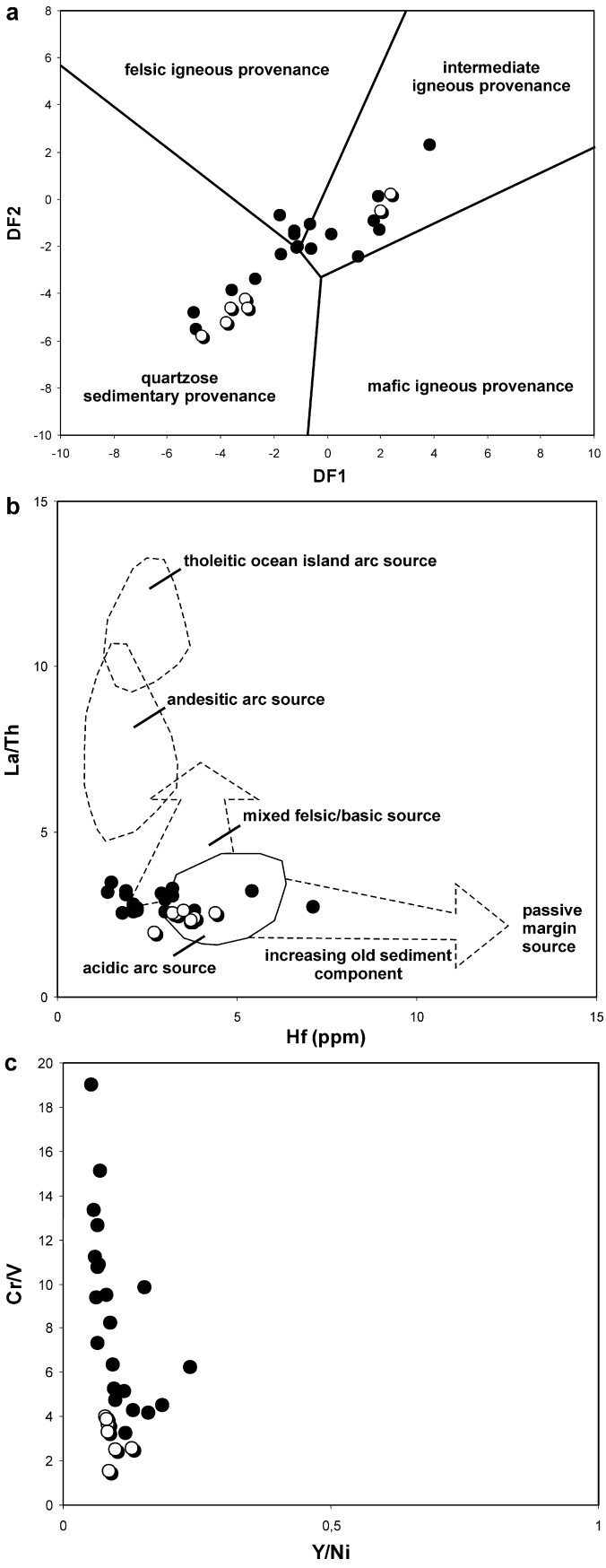

Fig. 9. Discrimination diagrams illustrating sedimentary provenance: a) Discriminant function (DF) analysis using major elements after Roser and Korsch (1988). b) La/Th vs. Hf diagram after Floyd and Leveridge (1987). c) Cr/V vs. Y/Ni diagram after Hiscott (1984) and McLennan et al. (1993). Black dots: sandstones, white dots: mudstones.

Author's personal copy

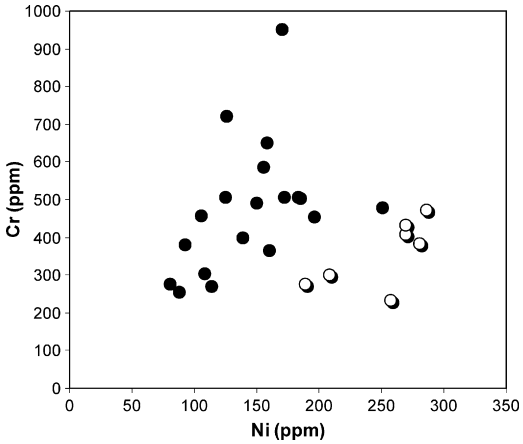

Fig. 10. Correlation diagram of Cr vs. Ni abundances for the studied Karpathos samples. Black dots: sandstones, white dots: mudstones.

rocks. Especially for the LaN/YbN ratio, Bhatia (1985) proposed: 1) for passive margins: ca. 10.8, 2) for Andean type continental margins (active continental margins): ca. 8.5, 3) for continental island arcs: ca. 7.5 ± 2.5, 4) for oceanic island arcs: ca. 2.8 ± 0.9. The studied sediments show an average LaN/YbN ratio of ≈7. Taking into account the above parameters, a continental island arc setting is the most probable setting for all the analyzed sandstones.

5. Discussion

5.1. Petrographical results

Modal analysis of the studied Karpathos turbidite sandstones suggests that the sediments were derived from sedimentary, igneous (plutonic and volcanic) and metamorphic rock sources. The latter source is pointed by the presence of microcline and metamorphic lithoclasts and the occurrence of metamorphic heavy minerals such as rutile, which is a widespread accessory mineral in metamorphic rocks, and tourmaline, which is abundant in granites and region and contact metamorphic rocks (Mange and Maurer, 1991). Igneous rock source seems to consist mainly by felsic plutonic granite and mafic volcanic basalt. Basalt fragments, along with the occurrence of serpentinite, dolerite and chromium spinels, indicate a possible ophiolitic provenance. The studied sandstones exhibit high percentages of lithic fragments and matrix, medium to low quartz content and presence of medium to poorly-sorted angular to subangular framework grains. These features are indicative of compositionally immature sandstones. On the QFL triangular diagram, the sandstones plot around the boundary between the recycled orogenic and the dissected magmatic arc field (Fig. 5), an observation which indicates a possible mixing of sediment from an eroded, mature magmatic arc and from quartzose, recycled sources. These observations indicate that (1) the depositional environment was relatively close to the source rocks and (2) the source rocks may be of two types, a continental source (responsible for the quartz and low-grade metamorphic fragments) and a volcanic-arc source (responsible for the amounts of plagioclase and volcanic fragments).

5.2. Geochemical results

The geochemical classification of most sandstones as immature wackes and litharenites (Herron, 1988) is in agreement with petrographical observations. Cr/V vs. Y/Ni and Cr–Ni signatures confirm the existence of an ophiolitic sediment source indicated by petrography. Low Th/U vs. Th abundances indicate provenance from mantle-derived igneous rocks of depleted nature. The source rocks were slightly affected by weathering and sediment recycling, indicated by low Th/U and moderate Zr/Sc ratios. The latter observation probably indicates that the depositional environment was relatively close to the source rocks. The observed enrichment in LREE and the absence of significant negative Eu anomalies suggest derivation chiefly from young undifferentiated arc material with contribution from old upper continental crust (McLennan et al., 1993). The absence of significant negative Eu anomalies also indicate that intracrustal differentiation processes such as partial melting or fractional crystallization, involving separation of plagioclase, were not of great importance (McLennan, 1989; McLennan et al., 1990).

5.3. Tectonic setting

The preservation of detrital material of plutonic, volcanic, sedimentary and metamorphic origin in the same strata is indicative of only a minor weathering and sorting influence acting on the detritus on its way from the sediment source to the depositional basin. In turn, this implies (1) relatively short transport paths and thus potentially marked relief; and (2) only minor intermediate storage of sediment. These features are typical of tectonically active basins at active continental margins or of strike-slip basins (Nilsen and Sylvester, 1995; Zimmermann and Bahlburg, 2003). The most reasonable geotectonic setting that accommodates all these sediment sources is continental basins formed in the back-arc region, i.e. back-arc, strike-slip and foreland basins (Condie et al., 1992; Asiedu et al., 2000). According to the REE parameters of Bhatia (1985) and the discriminant diagrams of Bhatia and Crook (1986), almost all sandstones appear to have been deposited predominantly in a continental island arc setting (Fig. 12). A continental island arc is by definition an 'island arc formed on well-developed continental crust or on thin continental margin' with a provenance of a 'dissected magmatic arc-recycled orogen' (Bhatia and Crook, 1986). The latter observation confirms the agreement between petrographical and geochemical results, regarding the tectonic setting of the sedimentary basin.

5.4. Possible source areas

The occurrence of marble, schist, gneiss-augengneiss and quartzite fragments indicates a possible metamorphic source area composed by a continental basement core. The nearest metamorphic basement exposures in the area are: a) the pre-Alpidic metamorphic basement of eastern Crete (Franz et al., 2005; Zulauf et al., 2008), b) the pre-Alpidic metamorphic basement of the Dodecanese Islands Kalymnos, Leros and Lipsos (Franz et al., 2005) and c) the Menderes Massif of SW Turkey. The Menderes Massif is generally consisting of a crystalline gneissic "core" and a (meta)sedimentary cover of marbles and carbonate rocks and can be considered as a possible source of metamorphic detritus, but problems arise regarding the time in which the massif reached the surface, which probably is no earlier than the Early Miocene (Bozcurt and Satir, 2000). The pre-Alpidic metamorphic basement of eastern Crete is consisting of similar lithologies with the observed metamorphic lithoclasts, but probably is excluded as a possible sediment source because it was shown that the basement rocks of eastern Crete and the Dodecanese Islands had different tectonic evolution during the Alpine orogeny (Franz et al., 2005). The pre-Alpidic metamorphic basement of the Dodecanese Islands remains an alternative source area which was affected by deformation caused by the Lycian nappe pile (Franz et al., 2005). Another possible metamorphic source proposed by this study could be a lost metamorphic terrain of considerable extent that probably existed in the south-central Aegean, relics of which are observed as isolated

Author's personal copy

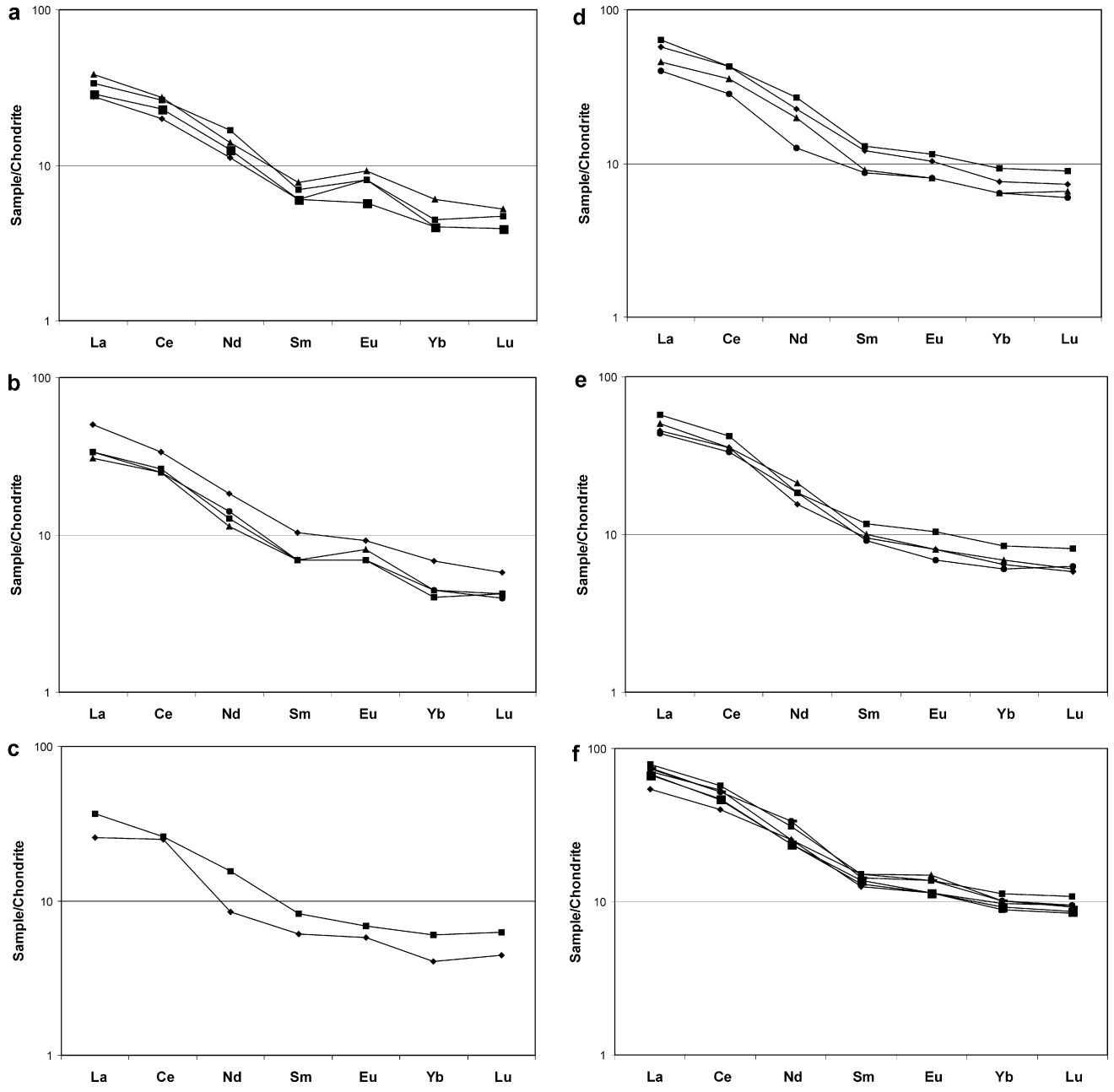

Fig. 11. Chondrite-normalized REE diagrams for Karpathos sandstones (a–e) and mudstones (f). Normalizing values from Taylor and McLennan (1985).

crystalline slices (consisting of metamorphic rocks, greenschists and granites) of Late Cretaceous age within the upper parts of the nappe piles in Crete and some Cycladic islands (Langosch et al., 2000; Garfunkel, 2004).

It is proposed that tectonic deformation caused by the Lycian Nappes affected the Dodecanese basement rocks (and probably the lost metamorphic terrain) leading to erosion of material which was incorporated in parts of the nappe pile and provided supply of sediment to Karpathos turbidites (Fig. 13). The latter hypothesis is strengthened by the following observations and data: a) presence of dolerite fragments in the studied thin sections, a possible source of which could be the dolerite dikes of Late Cretaceous age which intruded the ultramafic rocks that occur on top of the nappe piles in the Dodecanese Islands and the Taurides (Koepke et al., 2002), b) presence of marbles, schists, quartzites, serpentinites and basalts in the Lycian mélange and peridotite thrust sheet (Collins and Robertson, 1998, 1999), c) indications that the upper levels of the Lycian Nappes were subaerially exposed and eroded in Early Tertiary (Collins and Robertson, 1998).

5.5. Palaeogeographic speculations

Pantopoulos (2009) proposed that Karpathos turbidites were probably deposited in a foreland basin in front of an advancing nappe pile from the Early Eocene to Late Eocene–Early Oligocene. The style of nappe thrusting in Karpathos was described as thin-skinned (Harbury, 1986). Thin-skinned deformation is typical of many fold and thrust belts developed in the foreland of a collisional zone or back-arc of a continental volcanic arc. Since petrographical and geochemical results of this study propose a continental island arc tectonic setting, is possible that Karpathos turbidites were deposited in a retro-arc foreland basin, formed in the back-arc area of a continental arc. In the case that Karpathos Island is a part of the Anatolide-Tauride domain (Garfunkel, 2004) and the

Author's personal copy

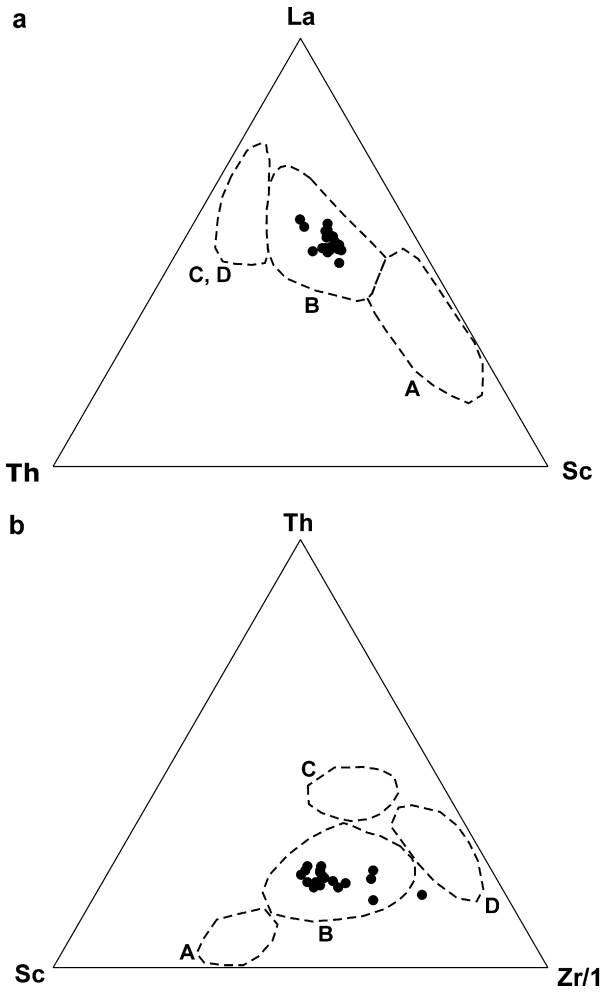

Fig. 12. Tectonic setting discrimination diagrams for Karpathos sandstones after Bhatia and Crook (1986). Oceanic island arc (A), continental island arc (B), active continental margin (C) and passive margin (D) fields are shown.

Lycian Nappes do extend into the Dodecanese Islands (Bernoulli et al., 1974), then the formation of this continental arc can be attributed to subduction of a branch of Neotethys beneath a continental fragment of the Anatolide domain in Early Tertiary times (Fig. 13). The latter hypothesis has significant similarities with the proposed model of Eocene flysch deposition in front of a thin-skinned Lycian nappe pile due to closure of the northern Neotethys ocean basin (Collins and Robertson, 1998; ten Veen et al., 2009).

A classic perception adopted in the literature is that Karpathos turbidite deposits probably represent a continuation of the Pindos foreland basin in the south-eastern Aegean. The Pindos foreland basin developed in the External Hellenides during the Late Cretaceous and Early Tertiary (Underhill, 1989), and comprises the Gavrovo and Ionian geotectonic zones (Aubouin, 1965). According to Underhill (1985) and Clews (1989), the subsidence was the result of lithospheric flexure, associated with thrust sheet loading, which took place in front of the Pindos thrust, during the Late Eocene to Oligocene. However, the connection of Karpathos turbidite deposits with the Pindos foreland remains problematic for the following reasons: a) age differences of about 15–20 million years in the onset of turbidite sedimentation which has a Late Eocene age in Ionian and Gavrovo Zones of western Greece (especially SW Greece) (Kamberis et al., 2000; Faupl et al., 2007; Konstantopoulos, 2009), a time in which turbidite sedimentation in Karpathos ended (Pantopoulos, 2009). An Early Eocene onset of turbidite sedimentation in the Ionian Zone was observed only in northwestern Greece near the Greek-Albanian borders (Avramidis and Zelilidis, 2001; Avramidis et al., 2002) with no similar onset age recorded elsewhere in the Gavrovo or Ionian Zones of southern Greece. Age similarities of Karpathos turbidites occur with the Pindos Zone turbidites (outcropping behind the Pindos thrust and incorporated to the Pindos nappe pile), the sedimentation of which seems to start in Maastrichtian-Paleocene or Early-Middle Eocene depending on the geographical position, but again problems occur regarding the differences between Pindos turbidites of northern and southern Greece: a large part of Pindos Zone turbidite sedimentation in southern Greece probably took place in a passive margin geotectonic setting and ended in Middle Eocene (Piper, 2006), b) occurrence of specific metamorphic lithic fragments (marble and augengneiss) in Karpathos turbidites which are not observed in western Greece, c) different Alpine evolution history between Crete and the Dodecanese Islands (Franz et al., 2005). The latter seem to have been affected by Tertiary deformation caused by the Lycian nappe pile (Bernoulli et al., 1974; Garfunkel, 2004; Franz et al., 2005).

6. Conclusions

Petrographic and geochemical analysis of Karpathos Island turbidites reveals that these sediments derived from igneous (plutonic–volcanic), sedimentary, low-grade metamorphic and ophiolitic sources. The turbidites are consisting of compositionally immature sandstones (wackes and litharenites) with high matrix content, that seem to have undergone minor degree of weathering and no significant sediment recycling. Petrography indicates a mixing of sediment from an eroded magmatic arc and from quartzose, recycled sources. Geochemical analysis is compatible with an

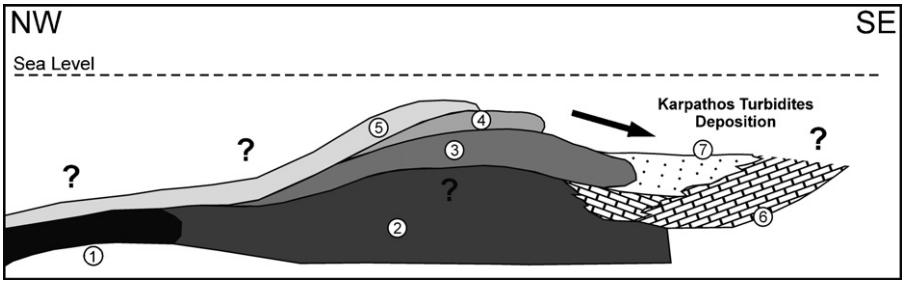

Fig. 13. Cross section schematizing the geotectonic environment of Karpathos turbidite sedimentation due to subduction of a Neotethys ocean basin branch during the Early Tertiary. 1 = Complete subducted oceanic lithosphere; 2 = Metamorphic basement of the Dodecanese Islands/Lost metamorphic terrain of southern Aegean; 3 = Lycian Nappes; 4 = Lycian Mélange (accretionary wedge); 5 = Ophiolitic nappes (Lycian Peridotite Thrust Sheet); 6 = Slope carbonates; 7 = Eocene turbidites; Magnitudes and distances are not to scale.

Modified from ten Veen et al. (2009) and based on reconstructions from Collins and Robertson (1999).

Author's personal copy

acidic to mixed felsic/basic source along with input of ultramafic detritus and recycling of older sedimentary components. REE data indicate provenance from young undifferentiated arc material with contribution from an old upper continental crust source. Turbidite sedimentation probably took place in a continental island arc setting as a result of subduction of a branch of Neotethys beneath a continental fragment of the Anatolide domain in Early Tertiary times. The relation of Karpathos turbidite deposits with the Pindos foreland basin (Gavrovo and Ionian Zones of western Greece) therefore becomes problematic.

Acknowledgments

This study was co-funded by E.U., European Social Fund and GSRT Greece, EPAN, PENED '03ED497. The authors would like to thank Assistant Professor Dr. B. Tsikouras and Mr. P. Balasis (University of Patras, Department of Geology, Section of Earth Materials) for their help with petrography and thin section preparation respectively. Constructive comments and suggestions by the editor-in-chief and an anonymous reviewer improved an initial version of the manuscript.

References

Asiedu, D.K., Suzuki, S., Shibata, T., 2000. Provenance of sandstones from the Lower Cretaceous Sasayama Group, Inner Zone of Southwest Japan. Sedimentary Geology 131, 9–24.

Aubouin, J., 1965. Geosynclines. Elsevier, Amsterdam.

Aubouin, J., Bonneau, M., Davidson, J., 1976. Contribution a la geologie de l'arc egeen: l'ile de Karpathos. Bulletin of the Geological Society of France 7 XVIII (2), 385–401.

Avramidis, P., Zelilidis, A., 2001. The nature of deep-marine sedimentation and palaeocurrent trends as an evidence of Pindos foreland basin fill conditions. Episodes 24 (4), 252–256.

Avramidis, P., Zelilidis, A., Vakalas, I., Kontopoulos, N., 2002. Interaction between tectonic activity and eustatic sea-level changes on basin evolution and hydrocarbon potential: the Pindos foreland and Mesohellenic piggy-back basins, central Greece. Journal of Petroleum Geology 25 (1), 53–82.

Basu, A., Young, S., Suttner, L., James, W., Mack, G., 1975. Re-evaluation of the use of undulatory extinction and crystallinity in detrital quartz for provenance interpretation. Journal of Sedimentary Petrology 45, 873–882.

Bernoulli, D., De Graciansky, P.C., Monod, O., 1974. The extension of the Lycian Nappes (SW Turkey) into the southeastern Aegean islands. Eclogae Geologicae Helveticae 67, 39–90.

Bhatia, M.R., 1985. Rare earth element geochemistry of Australian Paleozoic graywackes and mudstones: provenance and tectonic control. Sedimentary Geology 45, 97–113.

Bhatia, M.R., Crook, K.A.W., 1986. Trace element characteristics of graywackes and tectonic setting discrimination of sedimentary basins. Contributions to Mineralogy and Petrology 92, 181–193.

Blatt, H., Middleton, G., Murray, R., 1980. Origin of Sedimentary Rocks, 2nd ed. Prentice-Hall, Englewood Cliffs, NJ.

Bonneau, M., 1984. Correlation of the Hellenide nappes in the southeast Aegean and their tectonic reconstruction. In: Dixon, J.E., Robertson, A.H.F. (Eds.), The Geological Evolution of the Eastern Mediterranean. Geological Society of London, Special Publications 17, pp. 517–527.

Bozcurt, E., Satir, M., 2000. The southern Menderes Massif (western Turkey): geochronology and exhumation history. Geological Journal 35, 285–296.

Burnett, D.J., Quirk, D.G., 2001. Turbidite provenance in the Lower Paleozoic Manx Group, Isle of Man: implications for the tectonic setting of Eastern Avalonia. Journal of the Geological Society of London 158, 913–924.

Christodoulou, G., 1963. Geological map of Greece. Scale 1:50.000, Karpathos Island Sheets (Northern and Southern part). IGME, Athens, Greece, 2 folds map.

Clews, J., 1989. Structural controls on basin evolution: Neogene to Quaternary of the Ionian zone of western Greece. Journal of the Geological Society of London 146, 447–457.

Collins, A.S., Robertson, A.H.F., 1998. Processes of Late Cretaceous to Late Miocene episodic thrust-sheet translation in the Lycian Taurides, SW Turkey. Journal of the Geological Society of London 155, 759–772.

Collins, A.S., Robertson, A.H.F., 1999. Evolution of the Lycian Allochthon, western Turkey, as a north facing Late Palaeozoic to Mesozoic rift and passive continental margin. Geological Journal 34, 107–138.

Condie, C.K., Noll Jr., P.D., Conway, C.M., 1992. Geochemical and detrital mode evidence for two sources of Early Proterozoic sedimentary rocks from the Tonto Basin Supergroup, central Arizona. Sedimentary Geology 77, 51–76.

Crook, K.A.W., 1974. Lithogenesis and geotectonics: the significance of compositional variations in flysch arenites (graywackes). In: Dott, J.R., Shaver, R.H. (Eds.), Modern and Ancient Geosynclinal Sedimentation. SEPM Special Publications no. 19, Tulsa, Oklahoma, USA, pp. 304–310.

Davidson-Monett, J., 1974. Contribution a l'etude geologique de l'arc egeen: l'ile de Karpathos (Dodecanese meridional, Grece). PhD Thesis, Trav. Dept. Geol. Paris.

Dickinson, W.R., 1970. Interpreting detrital modes of graywacke and arkose. Journal of Sedimentary Petrology 40, 695–707.

Dickinson, W.R., Suczek, C.A., 1979. Plate tectonics and sandstone composition. AAPG Bulletin 63, 2164–2182.

Dickinson, W.R., Beard, L.S., Brakenridge, G.R., Erjavec, J.L., Ferguson, R.C., Inman, K.F., Knepp, R.A., Lindberg, F.A., Ryberg, P.T., 1983. Provenance of North American Phanerozoic sandstones in relation to tectonic setting. Geological Society of America Bulletin 94, 222–235.

Faupl, P., Pavlopoulos, A., Migiros, G., 2007. Provenance of flysch sediments and the Paleogene-Early Miocene geodynamic evolution of the Hellenides: a contribution from heavy mineral investigations. In: Mange, M.A., Wright, D.T. (Eds.), Heavy Minerals in Use. Developments in Sedimentology, vol. 58, pp. 765–788.

Floyd, P.A., Leveridge, B.E., 1987. Tectonic environment of the Devonian Gramscatho basin, south Cornwall: framework mode and geochemical evidence from turbidite sandstones. Journal of the Geological Society of London 144, 531–542.

Folk, R.L., 1974. Petrology of Sedimentary Rocks, 2nd ed. Hemphill Press, Austin, Texas.

Franz, L., Okrusch, M., Seidel, E., Kreuzer, H., 2005. Polymetamorphic evolution of pre-Alpidic basement relics in the external Hellenides, Greece. Neues Jahrbuch für Mineralogie-Abhandlungen 181, 147–172.

Fytrolakis, N., 1989. Contribution to the knowledge of the pre-Neogene of Karpathos. Bulletin of the Geological Society of Greece 23 (1), 119–130.

Gao, S., Wedepohl, K.H., 1995. The negative Eu anomaly in Archean sedimentary rocks: implication for decomposition, age and importance of their granitic sources. Earth and Planetary Science Letters 133, 81–94.

Garfunkel, Z., 2004. Origin of the Eastern Mediterranean basin: a reevaluation. Tectonophysics 391, 11–34.

Garver, J.I., Royce, P.R., Smick, T.A., 1996. Chromium and nickel in shale of the Taconic foreland: a case study for the provenance of fine-grained sediments with an ultramafic source. Journal of Sedimentary Research 66, 100–106.

Harbury, N.A., 1986. The stratigraphy and structural evolution of the SE Aegean. PhD Thesis, University of London.

Harbury, N.A., Hall, R., 1988. Mesozoic extensional history of the southern Tethyan continental margin in the SE Aegean. Journal of the Geological Society of London 145, 283–301.

Hatzipanagiotou, K., 1983. Die oberste Einheit des sud-agaischen Deckenstapels auf Rhodos und Karpathos (Dodecanes/Griechenland)-Relikte eines Ophiolith-Komplexes. PhD Thesis, Technischen Universitat Braunschweig.

Herron, M.M., 1988. Geochemical classification of terrigenous sands and shales from core or log data. Journal of Sedimentary Petrology 58, 820–829.

Hiscott, R.N., 1984. Ophiolitic source rocks for Taconic-age flysch: trace-element evidence. Geological Society of America Bulletin 95, 1261–1267.

Hoffman, E.L., 1992. Instrumental neutron activation in geoanalysis. Journal of Geochemical Exploration 44, 297–319.

Ingersoll, R.V., Bullard, T., Ford, R., Grimm, J., Pickle, J., Sares, S., 1984. The effect of grain size on detrital modes: a test of the Gazzi-Dickinson point-counting method. Journal of Sedimentary Petrology 54, 103–116.

Kamberis, E., Sotiropoulos, S., Aximniotou, O., Tsaila-Monopoli, S., Ioakim, C., 2000. Late Cenozoic deformation of the Gavrovo and Ionian zones in NW Peloponnesus (Western Greece). Annali di Geofisica 43, 905–919.

Koepke, J., Seidel, E., Kreuzer, H., 2002. Ophiolites on the Southern Aegean islands Crete, Karpathos and Rhodes: composition, geochronology and position within the ophiolite belts of the Eastern Mediterranean. Lithos 65, 183–203.

Kokkalas, S., Doutsos, T., 2004. Kinematics and strain partitioning in the southeast Hellenides (Greece). Geological Journal 39, 121–140.

Konstantopoulos, P., 2009. Depositional environments and stratigraphic arrangement of the Peloponnesus flysch. Possible hydrocarbon generation. PhD Thesis, University of Patras.

Langosch, A., Seidel, E., Stosch, H.G., Okrusch, M., 2000. Intrusive rocks in the ophiolitic melange of Crete-Witnesses to a Late Cretaceous thermal event of enigmatic geological position. Contributions to Mineralogy and Petrology 139, 339–355.

Mange, M.A., Maurer, F.W., 1991. Heavy Minerals in Colour. Enke-Verlag, Stuttgart.

McLennan, S.M., 1989. Rare earth elements in sedimentary rocks: influence of provenance and sedimentary process. In: Lipin, B.R., McKay, G.A. (Eds.), Geochemistry and Mineralogy of Rare Earth Elements. Mineralogical Society of America, Washington, Reviews in Mineralogy no. 21, pp. 169–200.

McLennan, S.M., Taylor, S.R., McCulloch, M.T., Maynard, J.B., 1990. Geochemical and Nd-Sr isotopic composition of deep-sea turbidites: crustal evolution and plate tectonic associations. Geochimica et Cosmochimica Acta 54, 2015–2050.

McLennan, S.M., Hemming, S., McDaniel, D.K., Hanson, G.N., 1993. Geochemical approaches to sedimentation, provenance and tectonics. In: Johnsson, M.J., Basu, A. (Eds.), Processes Controlling the Composition of Clastic Sediments. Geological Society of America Special Paper no. 284, pp. 21–40.

Meinhold, G., Kostopoulos, D., Reischmann, T., 2007. Geochemical constrains on the provenance and depositional setting of sedimentary rocks from the islands of Chios, Inousses and Psara, Aegean Sea, Greece: implications for the evolution of Palaeotethys. Journal of the Geological Society of London 164, 1145–1163.

Nesbitt, H.W., Markovics, G., Price, R.C., 1980. Chemical processes affecting alkalis and alkaline earths during continental weathering. Geochimica et Cosmochimica Acta 44, 1659–1666.

Nilsen, T.H., Sylvester, A.G., 1995. Strike-slip basins. In: Busby, C.J., Ingersoll, R.V. (Eds.), Tectonics of Sedimentary Basins. Blackwell Science, Oxford, pp. 425–457.

Author's personal copy

Pantopoulos, G., 2009. Depositional environments, stratigraphic arrangement and bed thickness statistical analysis of Karpathos Island turbidite deposits. Possibility for the development of hydrocarbon plays in the SE Aegean. PhD Thesis, University of Patras.

Pettijohn, F.J., Potter, P.E., Siever, R., 1972. Sand and Sandstone. Springer-Verlag, New York.

Piper, D.J.W., 2006. Sedimentology and tectonic setting of the Pindos flysch of the Peloponnese, Greece. In: Robertson, A.H.F., Mountrakis, D. (Eds.), Tectonic Development of the Eastern Mediterranean Region. Geological Society of London, Special Publications, 260, pp. 493–505.

Roser, B.P., Korsch, R.J., 1988. Provenance signatures of Sandstone–Mudstone suites determined using discriminant function analysis of major-element data. Chemical Geology 67, 119–139.

Seidel, E., Wachendorf, H., 1986. Die südägäische Inselbrücke. In: Jacobshagen, V. (Ed.), Geologie von Griechenland. Borntraeger, Berlin, pp. 54–80.

Taylor, S.R., McLennan, S.M., 1985. The Continental Crust: Its Composition and Evolution. Blackwell Scientific, Oxford.

ten Veen, J.H., Boulton, S.J., Alçiçek, M.C., 2009. From palaeotectonics to neotectonics in the Neotethys realm: the importance of kinematic decoupling and inherited structural grain in SW Anatolia (Turkey). Tectonophysics 473, 261–281.

Tortosa, A., Palomares, M., Arribas, J., 1991. Quartz grain types in Holocene deposits from the Spanish central system: some problems in provenance analysis. In: Morton, A.C., Todd, S.P., Haughton, P.D.W. (Eds.), Developments in Sedimentary Provenance Studies. Geological Society of America Special Paper no. 57, pp. 47–54.

Underhill, J.R., 1985. Neogene and quaternary tectonics and sedimentation in Western Greece. PhD Thesis, University of Wales, Cardiff.

Underhill, J.R., 1989. Late Cenozoic deformation of the Hellenide foreland, western Greece. Geological Society of America Bulletin 101, 613–634.

Weber, J.N., Middleton, G.V., 1961a. Geochemistry of the turbidites of the Normanskill and Charney formations-I: effect of turbidity currents on chemical differentiation of turbidites. Geochimica et Cosmochimica Acta 22, 200–243.

Weber, J.N., Middleton, G.V., 1961b. Geochemistry of the turbidites of the Normanskill and Charney formations-II: distribution of trace elements. Geochimica et Cosmochimica Acta 22, 244–288.

Zimmermann, U., Bahlburg, H., 2003. Provenance analysis and tectonic setting of the Ordovician clastic deposits in the southern Puna Basin, NW Argentina. Sedimentology 50, 1079–1104.

Zulauf, G., Klein, T., Kowalczyk, G., Krahl, J., Romano, S.S., 2008. The Mirsini Syncline of eastern Crete, Greece: a key area for understanding pre-Alpine and Alpine orogeny in the eastern Mediterranean. Zeitschrift der Deutschen Gesellschaft für Geowissenschaften 159 (3), 399–414.